Paweł DAWIDOWSKI[1], Kacper SOWA[2], Mariusz STOSUR[1], Marcin SZEWCZYK[1], Wojciech PIASECKI[1], Przemysław BALCEREK[1]

ABB Corporate Research Center - Poland (1), AGH University of Science and Technology (2)

Impact of power-cable length on operation of NPC inverter fed induction motor drive for various LC filter topologies

Abstract. *This paper presents detailed analysis of phenomena which occur in cable connection between the drive and the motor. The impact of cable length on the proper inverter operation as well as protection against additional stress of motor caused by reflection in cable is analyzed, on a model developed for this purpose. Several configurations of output LC filters were implemented to investigate the optimal solution to reduce transient effect caused by dv/dt and high order harmonics.*

Streszczenie. *W artykule przedstawiono analizę zjawisk występujących w układzie zasilania silnika indukcyjnego z trójpoziomowego falownika napięcia poprzez linię kablową. Zbadano wpływ długości linii kablowej na przebiegi wyjściowe falownika dla różnych konfiguracji filtra. Celem badań było ustalenia topologii filtra zapewniającej uniwersalność rozwiązania napędu przekształtnikowego, a zarazem eliminującej niekorzystne zjawiska występujące w tego typu układach. (**Wpływ długości kabla na pracę trójpoziomowego falownika NPC zasilającego silnik indukcyjny dla różnych konfiguracji filtrów LC**).*

Keywords: NPC inverter, cable connection, voltage reflections, LC filter.
Słowa kluczowe: trójpoziomowy falownik napięcia, połączenie kablowe, odbicia fali elektromagnetycznej, filtr LC.

Introduction

In many applications, a long connection between the inverter and the motor is required to achieve an optimal solution of constructions and environmental requirements. Therefore, a cable connection is required to energize distant electric devices. On the other hand, additional consequences take place where long power cables are employed such as: premature failure of motor winding insulation, early bearing failure and wave reflections [1, 2].

Wide range of applications in high-power and medium-voltages drive units utilize three-level neutral point clamped (3L-NPC) inverters. The basic circuit diagram of such inverter is presented in Fig. 1. In the paper such solution will be taken into further consideration. The main features of these types of devices are reduced dv/dt and relatively low THD levels in comparison with the two-level inverters.

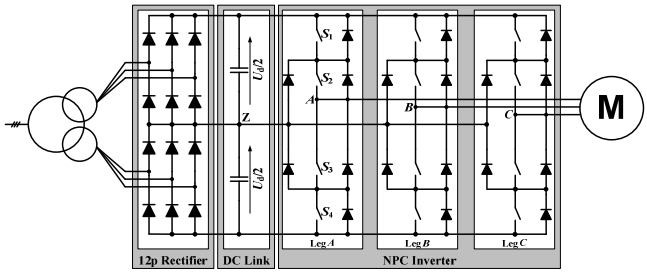

Fig.1. NPC Three-level inverter feeding the induction motor drive

Drive topology depicted in Fig. 1 is composed of a 12-pulse diode rectifier fed by a phase-shifting transformer with two secondary windings, Wye and Delta connected. It is an optimal solution considering costs and the reduction of a high level of current harmonics compared to the distortions caused by 6-pulse diode rectifier. Such passive rectifier does not allow for regenerative braking or four-quadrant operation. It is only able to deliver power from the AC network to the DC link, but not vice versa [3]. In Fig. 1 point Z of the diode rectifier is connected to the neutral point of the NPC inverter. Such connection ensures that total DC voltage is equally divided between two DC link capacitors [4] and is required for proper operation of the inverter.

The NPC inverter consists of three branches (A, B, C). Each branch consists of four switches marked as S_1 to S_4 connected in parallel with diodes as presented in Fig. 1.

Waveforms generated by PWM inverters have negative impact on motors and cables. They cause several problems such as the ones listed in [5]:

1. High dv/dt of the inverter output voltage causes reflections in the cable. This may increase motor terminal voltage up to the double value;
2. Additional losses in the motor;
3. Motor winding insulation degradation;
4. Electromagnetic emission caused by high dv/dt;
5. Harmonic currents can flow through stray capacitance in motor bearings causing their failure.

Selected drive topology naturally reduces reflections caused by high dv/dt. Yet this issue still exists in a limited form and plays significant role especially for “critical cables lengths”. Therefore the analysis of these effects is needed in order to achieve the required level of efficiency and ensure long lifetime of the installation. Several papers demonstrate the importance of this issue [6-9].

To study these phenomena a model of three-level NPC inverter has been developed in MATLAB SIMULINK. Fundamental information regarding the inverter and the transient effects in cables is presented in next chapters. Simulation results obtained during the study show typical phenomena which occur in the examined circuit. Various combinations of LC filters were tested to mitigate the negative impact of the cable length on the output inverter waveforms. This study allows for determination of the optimal solution for different cable lengths.

Principle of NPC inverter operation

Detailed analysis of the NPC inverters can be found in [4, 10, 11]. Here, only the most important information will be briefly reviewed, to explain the nature of output waves generated by the inverter.

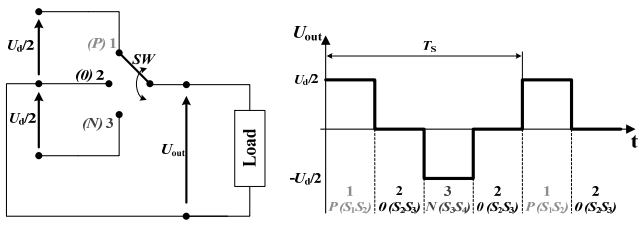

Fig.2. Principle of operation for single inverter leg

The basic principle of operation for a single inverter branch is illustrated in Fig. 2. Three states of operation are possible [10] (all of these switching operations occur in one period T_S and can be also observed in other inverter branches):

1. Switch *SW* is in position 1, $U_{out} = U_d/2$ (*P*-state);
2. Switch *SW* is in position 2, $U_{out} = 0$ (0-state);
3. Switch *SW* is in position 3, $U_{out} = -U_d/2$ (*N*-state).

In practice, according to Fig. 1, *P*-state is realized when switches S_1 and S_2 are turned on, switches S_3 and S_4 are turned off. State 0 when S_2 and S_3 are turned on, switches S_1 and S_4 are turned off. State *N* when S_3 and S_4 are turned on, switches S_1 and S_2 are turned off.

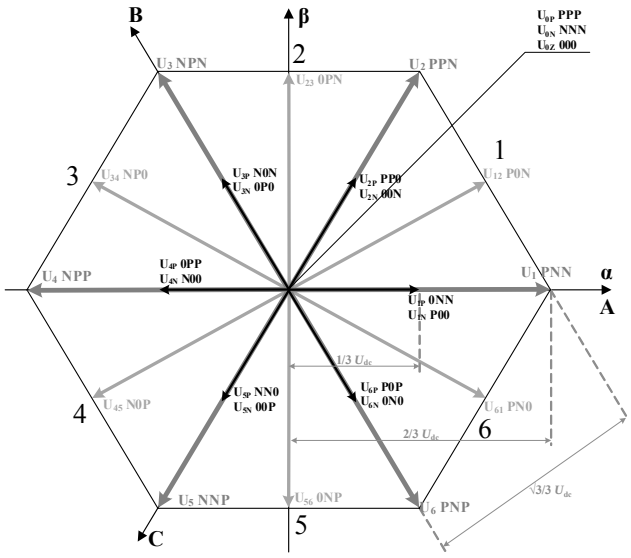

Fig.3. Space vector diagram of the three-level NPC inverter

As shown in Fig. 3, there are 27 switching states altogether (all combinations of *P*, 0 and *N*-states for each inverter branch) [12]:

$$n_{SW} = n^p = 3^3 = 27 \tag{1}$$

where: n – number of voltage levels, p – number of phases in the converter.

These 27 switching states produce only 19 unique voltage vectors, which can be classified into four voltage vectors groups: large, medium, small and zero. The plane can be divided into 6 major triangular sectors from 1 to 6 as marked in Fig. 3 each of which represents 60^0 of the fundamental cycle. Switching operations between these voltage vectors may cause several problems.

Reflections phenomena in power cables

The cable can be represented by an *RLC* pi model, where inductance, resistance and capacitance are distributed along the cable length [9], as illustrated in Fig. 4.

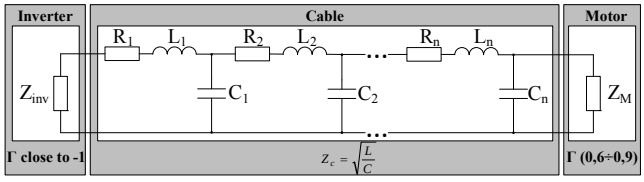

Fig.4. Equivalent circuit of cable, with typical values of reflections coefficients Γ

In the case of frequency increase the inductance and the capacitance impact on the traveling wave phenomena is greater than the impact of the resistance which is due to the skin effect. Presented simulations were performed for fixed resistance calculated at 50 Hz. This allows for simplification of the simulation process without compromising the accuracy.

The motor equivalent impedance is always larger compared to the cable impedance during steady state operation [1]. For higher than nominal frequencies this impedance can be considered as an open circuit, while the inverter behaves like the cable short circuited at its end [14]. Reflections occur when there is a mismatch between the cable surge impedance Z_c and the impedance at the end of the cable Z_{out} (in the case considered: Z_{inv} or Z_M) [1]. The reflection coefficient is:

$$\Gamma = \frac{Z_{out} - Z_c}{Z_{out} + Z_c} \tag{2}$$

Reflected voltage can be expressed as:

$$u_{ref} = \Gamma u_{in} \tag{3}$$

The voltage affecting the motor terminals is equal to:

$$u_{out} = u_{in} + u_{ref} \tag{4}$$

Fig. 5 illustrates the example where the propagation time t_p of the traveling wave is greater than half of the rising time t_r (full voltage reflection will take place).

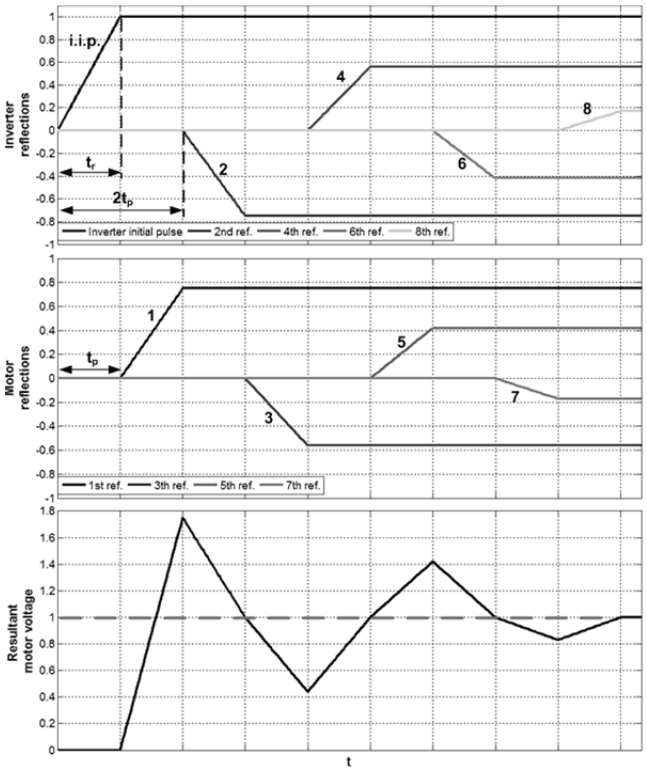

Fig.5. Voltages reflection in cable, observed on inverter and motor terminals [pu] (*inverter reflection coefficient* = -1; *motor reflection coefficient* = 0.75; $t_p = t_r$)

LC filters for inverter applications

The reflection phenomenon is closely related to the cable length, the magnitude of the DC link voltage and the switching frequency of the inverter, which determines *dv/dt*. LC filters are required to limit overvoltage at the cable and the motor terminals. This will cause the required limitation of undesirable harmonics and partly compensate the reactive power of the motor.

There are many LC filters design approaches presented in several papers, e.g. [13-15]. This paper is focused on evaluation of different filter topologies with various cable lengths. For all considered filter topologies L_f, C_f parameters will be identical. Filter resonance frequency is determined by:

$$f_r = \frac{1}{2\pi\sqrt{L_f C_f}} \tag{5}$$

In this paper filter parameters have been selected by taking into account the following facts:

1. Selected resonance frequency has to be above the fundamental frequency but below the lowest harmonic frequency [5]: factor 10 between fundamental/ resonance/switching frequency e.g. 50/500/5000 Hz;
2. An increase of switching frequency allows size reduction, thus reduction of weight and cost of filter components (due to the fact that the first group of harmonics is concentrated around twice the switching frequency);
3. If one considers (5) the L_f and C_f can be selected freely if their product is kept. Practically the capacitors are expected to be the easier option to realize than the chokes. Additionally, by increasing C_f the power rating of the inverter will be increased.

Experimental results

Studies were carried out utilizing MATLAB SIMULINK model presented in Fig. 6. The cable connection between drive and motor was modeled as a distributed parameters line (the Bergeron model, as described in [16]). This model appropriately represents traveling wave phenomena if high sampling ratio is set.

Alternatively one can utilize series PI sections line model. Yet, because such model has upper limit of frequency response depending on the number of PI sections, in the cases considered the Bergeron model will be selected [17].

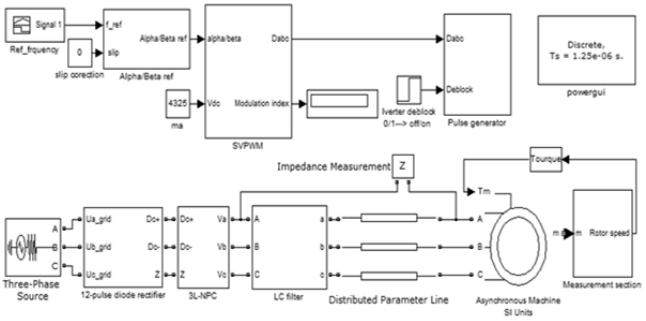

Fig.6. Block diagram of the model used during tests; connection of impedance scanner indicated

The impact of the cable length and the filter parameters on the output inverter waveforms was studied for several LC filter topologies based on [5] as shown in Fig. 7. The results of evaluation for different LC filter topologies are presented in Fig. 8. All filter configurations have been checked to determinate the lowest THD factor depending on the required cable length. Additionally parameters of passive filter components were optimally selected to minimize the filter size.

The results presented in Fig. 8 show that the lowest THD factors can be obtained by installing 1st or 6th filter configuration. Utilization of these filter topologies have several other advantages: a minimum number of elements is required (if one compare to 5th filter topology as presented in Fig. 7) and the voltage magnitude across capacitors is lower in comparison with 2nd the filter configuration). If one consider 6th filter its Wye point is connected to the DC link neutral point – *Z*. This ensures that the capacitors voltage does not exceed half of the DC link voltage magnitude.

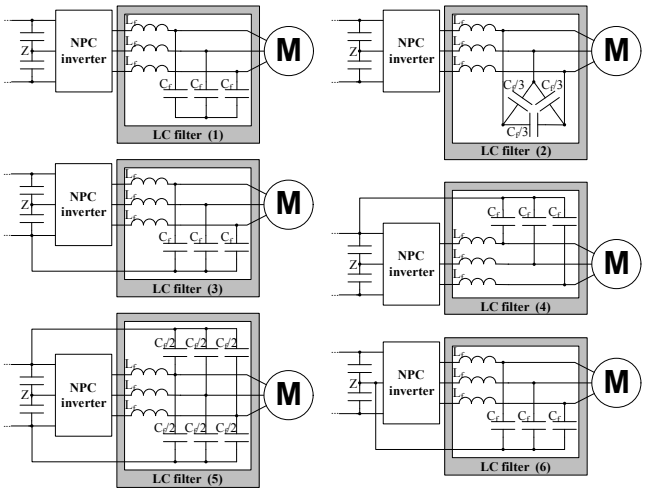

Fig.7. Examined LC filters topologies

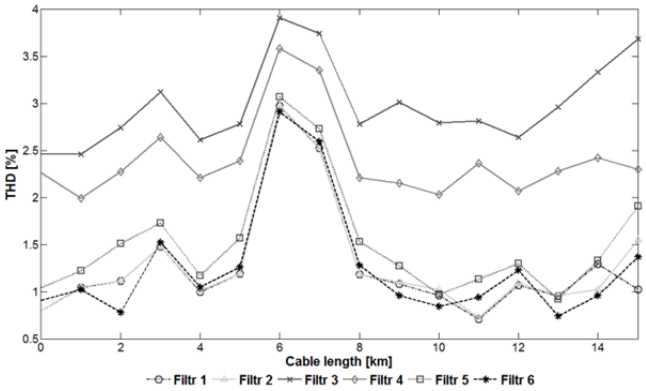

Fig.8. THD factor depending on cable length and selected filters configurations

Overall conclusion is the 6th filter configuration could be optimal if one utilize 6-pulse rectifier. 1st filter configuration is optimal if 12-pulse rectifier is utilized where *Z* – connection occurs. It should be noted that the common mode voltage (result of the switching action of the inverter and rectifier) can be transferred from the motor side to the secondary winding of the isolation transformer [18].

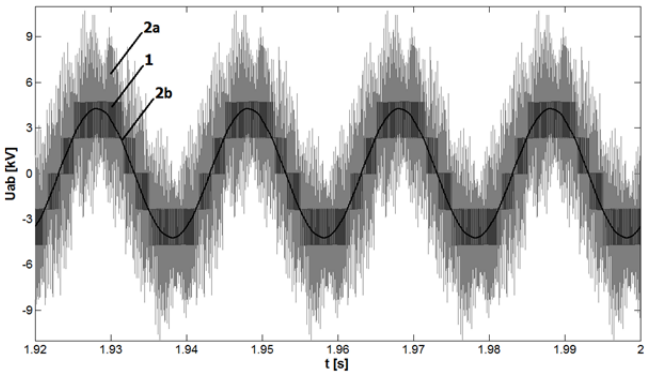

Fig.9. (1) Output phase-to-phase voltages U_{ab} measured at the inverter terminals, (2) voltage measured at motor terminals: (2a) without LC filter, (2b) with LC filter installed

Fig. 9 illustrates an exemplary output phase-to-phase voltages U_{ab} at the NPC inverter terminals and at the motor

terminals for 1th configuration of the LC filter (f_r = 500 Hz). The cable connection due to traveling wave phenomena caused voltages reflection as mentioned above. The voltage waveforms presented in Fig. 9 consider two cases: with and without LC filters installation.

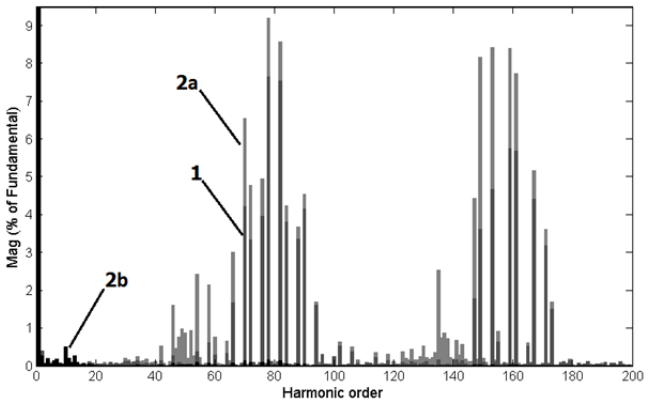

Fig.10. Harmonic spectrum of the voltage waveforms in Fig 9; $THD_{(1)}$=19.28%, $THD_{(2a)}$=33.75%, $THD_{(2b)}$=0.96%

Fig. 10 presents a comparison of U_{ab} voltages harmonic spectrums of the voltages shown in Fig. 9. A significant reduction of high order harmonics was obtained as expected. The required total harmonic distortion for the voltage below 69 kV is defined in [19] as 5% calculated for first 50 harmonics [20]. According to Fig. 11 appropriately selection of filter f_r ensures this requirement is fulfilled.

In accordance to the guidelines for LC filter design presented in the previous section, dumping capabilities of 1th filter configuration in Fig. 7 were examined for different resonance frequencies f_r, as presented in Fig. 11.

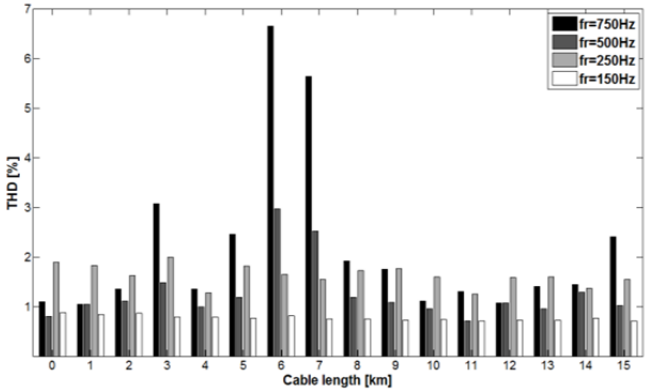

Fig.11. THD dependence on cable length for various resonance frequencies f_r for 1st filter configuration

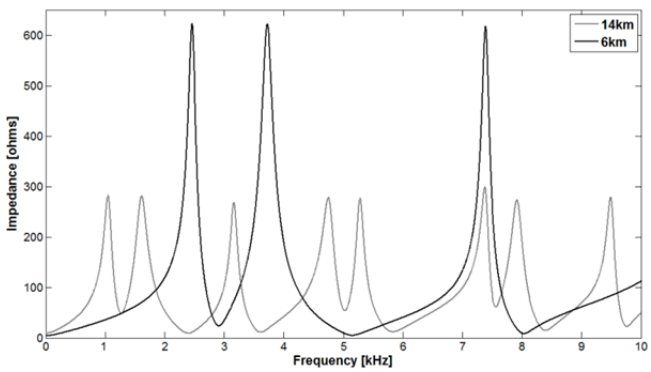

Fig.12. Impedance curves simulated for two cable lengths, with highest and lowest THD levels

For different f_r analyzed in Fig. 11 the decrease of the value of the filter resonance frequency causes reduction of THD level. Additionally fewer fluctuations were observed.

Fig. 12 presents the results of impedance frequency sweep, for one phase, calculated between the inverter and the motor terminals (as shown in Fig. 6 by Impedance Measurement block). Two cases are presented for filter f_r = 500 Hz, where the lowest and the highest THD level have been observed. In Fig. 12 one can observe, the longer cable local maxima are placed more densely than for the shorter one but they have lower magnitudes.

To limit the undesirable harmonic content one can select such switching frequency f_{sw} that the cable impedance is at one of the maximum values.

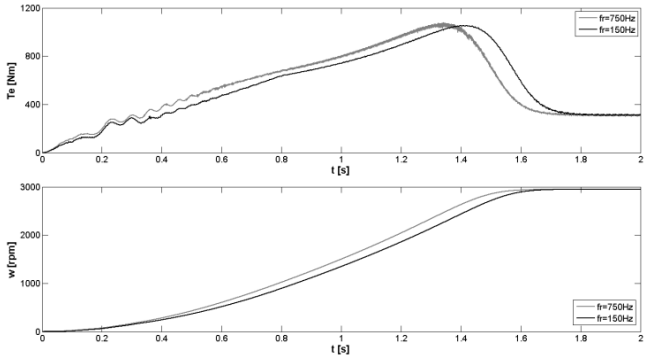

Fig.13. Measured curves of the electromagnetic torque and the rotor speed

As a result of this work the typical waveforms of induction machine were derived. Fig. 13 presents electromagnetic torque and rotor speed during the motor start-up process. Presented results are obtained for two resonance frequencies of the filter connected with a 10 km cable length. To the best of author's knowledge the filter installation limits torque oscillation and ripples. In this study the dependence of the cable length on the electromechanical torque can be observed.

Conclusions

In this paper the impact of various cable lengths on output waveforms produced by three-level NPC inverter feeding the induction motor drive has been investigated. Six filter configurations were examined to determine the most effective solution for damping harmonic components produced during the inverter operation. In all the cases the required level of THD factor, as defined according to [19], has not been exceeded when appropriate filter f_r was selected.

Out of the presented analyses, the filter configuration which offers best THD level can be taken for further considerations. All aspects have been examined to determine the optimal and possible operating condition, which provides proper operation of the whole system.

It has been noticed that the cable length will influence the selection of filter f_r. For some cable length it is possible to utilize higher f_r. This allows for installation of smaller components for LC filter.

Appendix

Table 1. Ratings and parameters of the induction machine [21]

P_N	kW	100
U_N	kV	3
f_N	Hz	50
ω_N	rpm	3000 (2963)
Poles	-	2
J	kg·m^2	2.7
T_N	Nm	322

Table 2. Parameters of filters

f_r [Hz]	C_f [mF]	L_f [mH]
750	0.1	0.45
500	0.1	1.00
250	0.4	1.00
150	1.0	1.10

Table 3. Ratings and parameters of the cable [22]

Cross section	mm^2	70
U_N	kV	10
C_L	μF/km	0.31
L_L	mH/km	0.41

Table 4. Measurement data to Fig. 8

Obtained values of THD [%]						
Length [km]	Filters configurations					
	1st	2nd	3rd	4th	5th	6th
0	0.80	0.80	2.46	2.26	1.04	0.91
1	1.04	1.05	2.46	1.99	1.22	1.02
2	1.11	1.11	2.74	2.27	1.51	0.78
3	1.48	1.48	3.12	2.64	1.73	1.52
4	1.00	1.01	2.61	2.21	1.17	1.05
5	1.19	1.19	2.78	2.39	1.57	1.26
6	2.97	2.98	3.91	3.58	3.07	2.91
7	2.52	2.53	3.74	3.35	2.73	2.59
8	1.18	1.18	2.78	2.21	1.53	1.28
9	1.08	1.10	3.01	2.15	1.27	0.96
10	0.96	1.02	2.79	2.03	0.97	0.84
11	0.71	0.72	2.81	2.36	1.13	0.94
12	1.07	1.09	2.64	2.07	1.30	1.23
13	0.95	0.96	2.96	2.28	0.92	0.74
14	1.29	1.02	3.33	2.42	1.33	0.96
15	1.02	1.55	3.68	2.30	1.91	1.37

REFERENCES

[1] Presson E., Transient Effect in Application of PWM Inverters to Industrial Motors, Conference Record of the *Annual IEEE Pulp and Paper Industry Technical Conference* (1991)

[2] Jouanne A., Enjeti P., Gray W., The effect of long motor leads on PWM inverter fed AC motor drive systems, *Applied Power Electronics Conference and Exposition Conference Proceedings* (1995), vol. 2, 592-597

[3] Electrical braking Technical guide no. 8, *ABB drives* (2011)

[4] Wu B., High-Power Converters and AC Drives, *Wiley-IEEE Press* (2006)

[5] Steinke J.K., Use of an LC Filter to Achieve a Motor-Friendly Performance of the PWM Voltage Source Inverter, *IEEE Transactions on Energy Conversion*, vol. 14 (1999), no. 1, 649-654

[6] Florkowska B., Florkowski M., Furgal J., Pajak P., Roehrich J., Zydroń P., Influence of fast switching phenomena on electrical insulation systems, *Przegląd Elektrotechniczny - Electrical Review, Warsaw, no 4,* (2010), 158-162

[7] Wlodek R. Roehrich J., Zydroń P., Analysis of overvoltage on motor winding insulation fed by PWM pulses, *High Voltage Engineering and Application (ICHVE), International Conference on*, (2010), 584-587

[8] Florkowska B., Zydroń P., Florkowski M., Effects of inverter pulses on the electrical insulation system of motors, *Industrial Electronics (ISIE), IEEE International Symposium on*, (2011) 573-578

[9] Cetin N.O., Hava A.M., Interaction between the filter and PWM units in the sine filter configuration utilizing three-phase AC motor drives employing PWM inverters, *Energy Conversion Congress and Exposition,* (2010), 2592-2599

[10] Piróg S., Power electronics: systems with network and hard commutations, *AGH Uczelniane Wydawnictwa Naukowo-Dydaktyczne*, (2006)

[11] Steinke J.K., Steimer P.K., Medium voltage drive converter for industrial applications in the power range from 0.5 MW to 5 MW based on a three-level converter equipped with IGCTs, PWM Medium Voltage Drives, no. 2000/063, *IEE Seminar* (2000), 1-4

[12] Corzine K.A., Baker J.R., Multilevel voltage-source duty-cycle modulation: analysis and implementation, *IEEE Transactions on Industrial Electronics*, vol. 49, no. 5, (2002), 1009-1016

[13] Finlayson P.T., Output filters for PWM drives with induction motors, *Pulp and Paper Industry Technical Conference* (1997) Annual, 186-193

[14] Jouanne A., Rendusara D.A., Enjeti P.N., Gray, J.W., Filtering techniques to minimize the effect of long motor leads on PWM inverter-fed AC motor drive systems, *IEEE Trans. on Industry Applications*, vol. 32, no. 4, (1996), 919-926

[15] Ahmed K.H., Finney S.J., Williams B.W., Passive Filter Design for Three-Phase Inverter Interfacing in Distributed Generation, *Compatibility in Power Electronics*, (2007),1-9

[16] SimPowerSystem Documentation: The Mathworks Inc. (2012)

[17] Mohamed K., Sid A.Z., Samir H., Mohammed K., Comparison of HVDC line models in PSB/SIMULINK based on steady-state and transients considerations, *Acta Electrotechnica et Informatica*, vol. 8, no. 2, (2008), 50-55

[18] Wei S., Zargari N., Wu B., Rizzo S., Comparison and Mitigation of Common-Mode Voltage in Power Converter Topologies, *IEEE Industry Applications Society (IAS) Conference* (2004), 1852-1857

[19] *IEEE Std 519-1992*, IEEE Recommended Practices and Requirements for Harmonic Control in Electrical Power Systems, Institute of Electrical and Electronics Engineers, Inc. (1993)

[20] *IEC 61000-4-7:2002*, Electromagnetic compatibility (EMC) - Part 4-7: Testing and measurement techniques- General guide on harmonics and interharmonics measurements and instrumentation, for power supply systems and equipment connected thereto (2002)

[21] High voltage Cast iron motors: Technical data for totally enclosed squirrel cage three phase motors, ABB (2011)

[22] XLPE Land Cable Systems- *User´s Guide*, ABB (2010)

***Authors**: Pawel Dawidowski Ph.D. Eng., Mariusz Stosur, Ph.D. Eng., Marcin Szewczyk, Ph.D. Eng., Wojciech Piasecki, Ph.D. Eng., Przemysław Balcerek, Ph.D. Eng. are with ABB Corporate Research Center, Starowiślna 13A Str., 31-038 Kraków, Poland, E-mails: pawel.dawidowski@pl.abb.com, mariusz.stosur@pl.abb.com, marcin.szewczyk@pl.abb.com, wojciech.piasecki@pl.abb.com, przemyslaw.balcerek@pl.abb.com, Kacper Sowa MSc Eng., AGH University of Science and Technology, 30 Mickiewicza Av., 30-059 Kraków, Poland, E-mail: sowa@agh.edu.pl*